# MASTERARBEIT / MASTER'S THESIS

Titel der Masterarbeit / Title of the Master's Thesis

## A geometric morphometric analysis of a Miocene freshwater fish assemblage from Schaßbach, Lavanttal Basin


verfasst von / submitted by

Felix Schult, BSc


angestrebter akademischer Grad / in partial fulfilment of the requirements for the degree of

Master of Science (MSc)

Wien, 2017 / Vienna, 2017

| | |
|---|---|
| Studienkennzahl lt. Studienblatt / degree programme code as it appears on the student record sheet: | A 066 831 |
| Studienrichtung lt. Studienblatt / degree programme as it appears on the student record sheet: | Masterstudium Zoologie |
| Betreut von / Supervisor: | Univ.-Prof. Dr. Jürgen Kriwet |

# Table of Content

Abstract ..... III
Abstract (Deutsch) ..... IV
Acknowledgements ..... V
Introduction ..... 1
Materials and Methods ..... 4
Results ..... 7
Discussion ..... 16
References ..... 21

# Abstract

The middle Miocene (16-14 Ma) fossil locality of Schaßbach, southern Austria within the Lavantal Basin, has provided skeletal remains of a freshwater fish assemblage. At least three different "freshwater" fish taxa are suggested for Schaßbach, namely *Gobius*, *Leuciscus* and *Morone*, although the latter is more a brackish water type. Most studies of bony fishes from the Lavanttal Basin are based on morphological characters like otoliths and teeth. In this study, the skeletal remains of the fish fossils in the assemblage were assessed by geometric morphometrics with the aims to (i) identify and separate the three suggested taxa for Schaßbach in the morphospace and (ii) describe the aspects of shape differentiates fishes in the assemblage. The shape analysis separated the fish assemblage into two clusters. Specimens within both clusters are randomly distributed, suggesting that they could be either from the same taxon or a family of closely related taxa. After identifying some of the specimens based on morphological key traits it became obvious that the fishes of the clusters belong to *Gobius* and *Leuciscus,* respectively. There is, however, at least one other taxon in the assemblage that does not belong to either of the three suggested taxa from Schaßbach but was grouped with *Leuciscus* because of a similar shape. The use of geometric morphometrics as a tool for taxon classification on assemblages of unknown taxa should be therefore questioned.



Keywords: geometric morphometrics; morphospace; Lavanttal; Miocene; fossil fish

# Abstract (Deutsch)

Aus der Fossil-Lokalität Schaßbach (mittleres Miozän; 16-14 Ma), südliches Österreich, im Lavanttaler Becken, wurde eine Sammlung aus fossilen Süsswasserfischen gesammelt. Mindestens Drei verschiedene „Süsswasser“ Fischtaxa werden in der Literatur für Schaßbach beschrieben, und zwar *Gobius*, *Leuscicus* und *Morone*, wobei letztere eher im Brackwasser vorkommen. Die meisten Studien über Knochenfische im Lavanttal basieren morphologischen Merkmale wie Otolithen oder Zähne – in dieser Studie hier, wurden vollständige fossile Fischreste mit verschiedene Methoden der geometrischen Morphometrie untersucht, mit dem Ziel (i) die drei beschriebenen Taxa im Morphoraum zu identifizieren und aufzutrennen und (ii) den Formunterschied, der zur Auftrennung der Fische in der Sammlung führt, zu beschreiben. Die Formanalyse der Fischsammlung hat jedoch nur zwei aufgetrennte Gruppen hervorgebracht. Fische beider Gruppen sind innerhalb der Gruppen zufällig verteilt, was vermuten lässt, dass sie zu einem Taxon oder eine Familie nah-verwandter Taxa gehören. Nachdem einige der Fische der Sammlung Anhand von morphologischer Schlüsselmerkmale identifiziert wurden, war klar, dass es sich bei den beiden Gruppen um jeweils *Gobius* und *Leuciscus* handelt. Jedoch gibt es mindestens ein anderes Taxon in der Sammlung, dass zu keinem der drei beschriebenen Taxa gehört, aber mit in der Gruppe von *Leuciscus* dazugezählt wurde, Aufgrund von ähnlicher Form. Der Nutzen der geometrischen Morphometrie als Werkzeug zur Klassifizierung von Taxa für Sammlungen aus unbekannten Arten, wird dadurch in Frage gestellt.

# Acknowledgements

I would like to thank Professor Jürgen Kriwet for making this Master thesis possible. I would like to thank my parents for their financial help and to my girlfriend Nicole Gierlinger as well as my brother Tony for all their love and support. Additionally, I would also like to thank Cheryl Gierlinger for proofreading my thesis.

# Introduction

The middle Miocene (ca. 16-14 Ma; Meller et al. 2015) fossil localty at Schaßbach, Lavanttal (= Lavant Valley) Basin, southern Austria (see Fig. 1), has provided skeletal remains of a fossil freshwater fish assemblage.

Plenty of other fossils have already been found, including insects, ostracods and rare remains of birds (Nolf & Brzobohatý 2009; Meller et al., 2015).

The fish remains at Schaßbach are suggested to belong to at least three different taxa, namely *Gobius* (Gobiidae) and *Leuciscus* (Cyprinidae), which are mostly freshwater types, and *Morone* (Moronidae), which live in brackish environments, but spawns in freshwater (Meller et al. 2015).

All these three “freshwater” fish taxa have also been described from other localities within the Lavanttal, including the non-marine “fish shale” of the Mühldorf Formation, which is situated southeast of the Schaßbach locality, Schönweg, Oberaigen and Fischering (Meller et al. 2015; Geologische Bundesanstalt Wien 2014a; Geologische Bundesanstalt Wien 2014b).

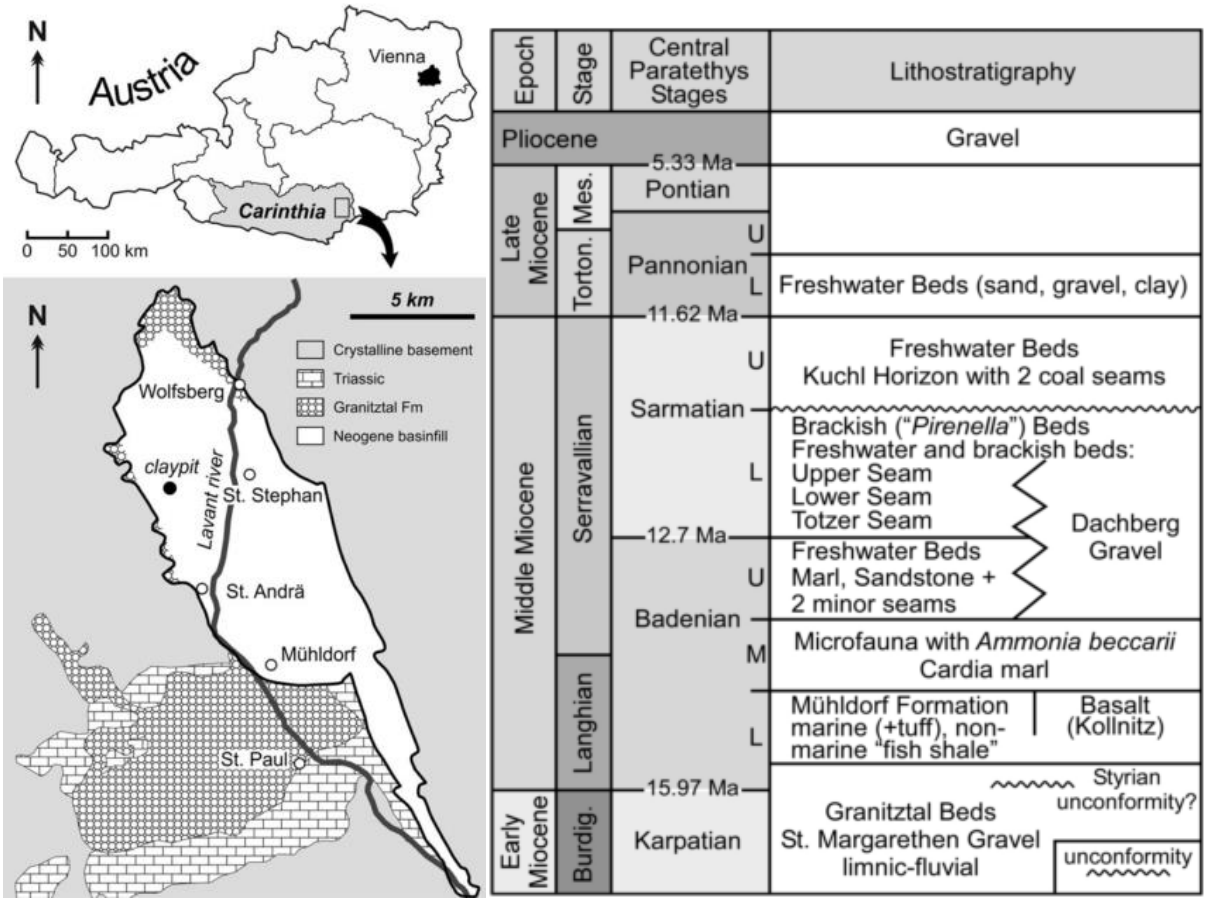

**Fig. 1 Geographic position of the Lavanttal Basin and the Schaßbach claypit.** (from Harzhauser et al. 2015, modified from Reischenbacher et al. 2007) and stratigraphy of the Neogene Lavanttal Basin (from Meller et al. 2015, based on Beck-Managetta 1952).

The Lavanttal itself, is a small pull-apart basin, formed during extrusion of crustal blocks towards the east in the southern part of the Eastern Alps. Paleogeographically, it lies in the western part of the Central Paratethys (Reischenbacher et al. 2007; Reischenbacher & Sachsenhofer 2013)

The Basin is downfaulted along the Pöls-Lavanttal Fault between the crystalline of the Sau- and Koralpe and started filling with thick fluvial gravels from the Granitztal Formation in the early Miocene (Karpatian, Burdigalian; ca. 17-16 Ma). The Granitztal Formation is succeeded by limnic sand, silt and clay from the lower non-marine "fish shale" Mühldorf Formation (lower Badenian; ca. 16-14.5 Ma; Meller et al. 2015; Harzhauser et al. 2015) and a younger marine sequence from the upper Mühldorf Formation, representing a marine ingression that reached the area during the Langhian (late early Badenian, 14.91 Ma; Reischenbacher et al. 2007; Harzhauser et al. 2015).

The Schaßbach fossil locality is situated at the western part in the center of the Lavanttal Basin. The sediments are considered to be of lacustrine and/or marine origin and early Badenian age (ca. 16-14 Ma). The outcrop is an active clay-pit with laminated and mica-bearing sand silt or clayey-sandy silts of grey to brown in colour (Harzhauser et al. 2015; Meller et al. 2015).

The lithology, fossil content and depositional environment in the sedimentary sequence of Schaßbach can be correlated with the non-marine "fish shale" from the lower part of the Mühldorf Formation (Harzhauser et al. 2015; Meller et al. 2015).

The lower Mühldorf Formation comprises lacustrine deposits that stem from a Miocene lake (Harzhauser et al. 2015). Reischenbacher et al. (2007) described it as a "shallow, quite lake with prevailing anoxic conditions and high sulfur contents suggesting a brackish influence".

However, fish layers near Mühldorf contain more sulfur than the layers at Schaßbach, indicating a more marine or brackish dominated influence at Mühldorf (Meller et al. 2015).

Most studies of bony fishes in the Lavantal Basin are based on otoliths and rarely by isolated teeth or skeletal remains (Nolf & Brzobohatý 2009). The fish skeletons here were assessed by geometric morphometrics, without identifying them beforehand with other methods. Landmarks (LM) were applied on the specimens to capture their overall body morphology in order to compare their shape. Differences and similarities were visualized by deformation grids and patterning in the morphospace.

These patterns of shape variation may act as a surrogate for different ecomorphotypes and provide new insight into the community structure, morphological diversity and the paleoecological framework

of freshwater fishes within the Lavanttal basin. Another aspect is that shape may also contain taxonomical information which can reflect phylogenetic relationships.

The specific aims of this study are to (i) identify and separate the three suggested taxa for Schaßbach based on geometric morphometrics (ii) describe which aspects of shape differentiates the fishes in the assemblage.

## Materials and Methods

The fossil fish specimens presented here were collected in 2013 on a student's excavation at the fossil locality Schaßbach *(46°47'52"N, 14°48'22"E)* in Carinthia, Austria. Fossils were mainly recovered from the surface and down to 1 m depth. The fish material is stored in the collection of the Department of Palaeontology, University of Vienna.

The fossil fishes were placed on a black background, next to a ruler with 1cm gradations. Then, specimens were all photographed with an Olympus digital camera in a lateral view and were mirrored with the head showing to the left side, if necessary, to allow homologous body position. The JPEG-image files were converted to TPS format using the software tpsUtil v.1.60. In total, 219 specimens were photographed but only 49 of them were used for the statistical analysis (for reasons see Discussion). Twelve landmarks were placed on every specimen image using the software tpsDig2 v. 2.18. These landmarks should represent biologically homologous anatomical loci (Zelditch et al. 2004). The selection of landmarks that were used (see Fig. 2) were based on, and is similar to, choices used in previous landmark studies of fishes (e.g. Klingenberg et al. 2003; Clabaut et al. 2007; Farré et al. 2016), but also on the accessibility of those landmarks on the majority of the specimens.

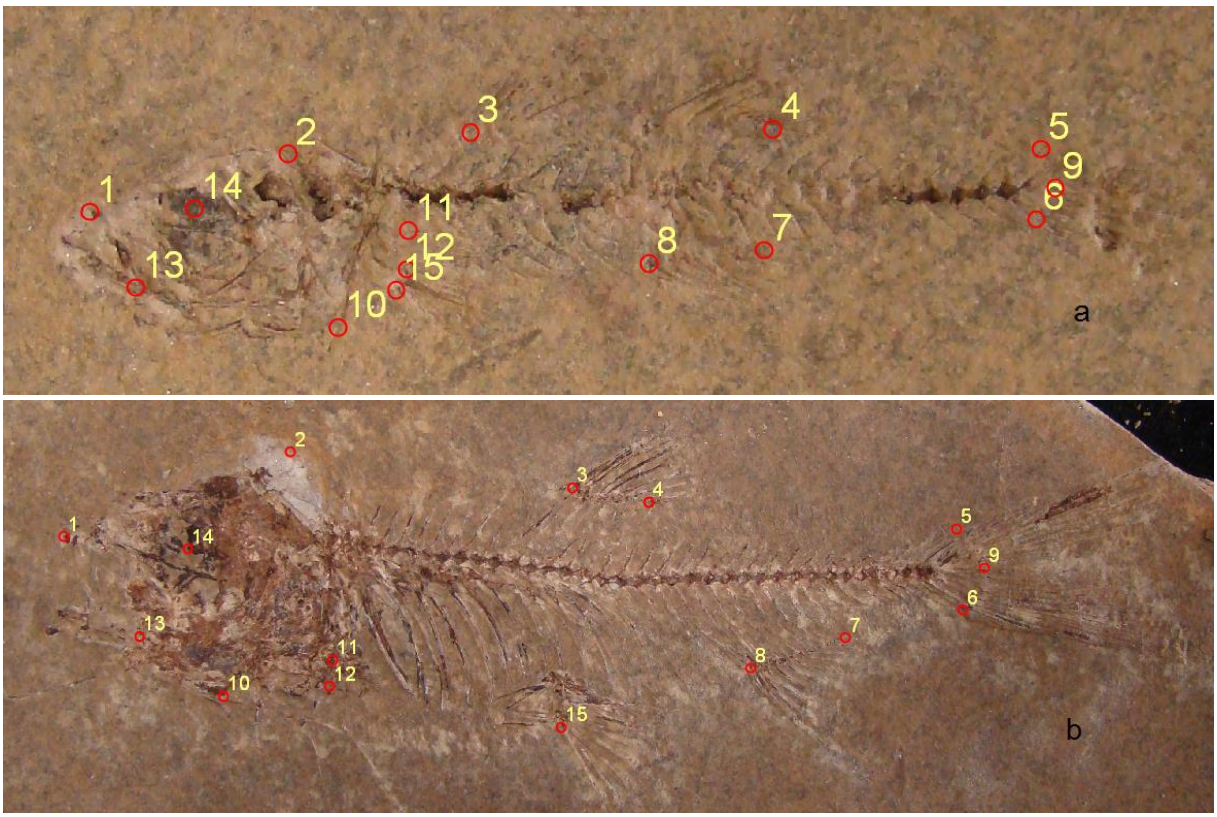


**Fig. 2 Example of landmark setting**. a. specimen with 2 dorsal fins; b. specimen with 1 dorsal fin

Landmarks were set as follows:

(1) snout tip, (2) dorsal margin of the end of the head, (3) anterior base of the dorsal fin (first dorsal fin if second fin exists), (4) posterior base of the dorsal fin (second dorsal fin if exists), (5) dorsal base of the caudal fin, (6) anterior base of the caudal fin, (7) anterior insertion of the anal fin, (8) posterior insertion of the anal fin , (9) posterior margin of the caudal peduncle, (10) ventral margin at the end of the head , (11) dorsal insertion of the pectoral fin, (12) ventral insertion of the pectoral fin, (13) corner of the mouth, (14) position of the eye, (15) anterior base of the pelvic fin

The primary aim was designated to reflect overall body morphology. Link files were created in tpsUtil v. 1.60 for better visualization.

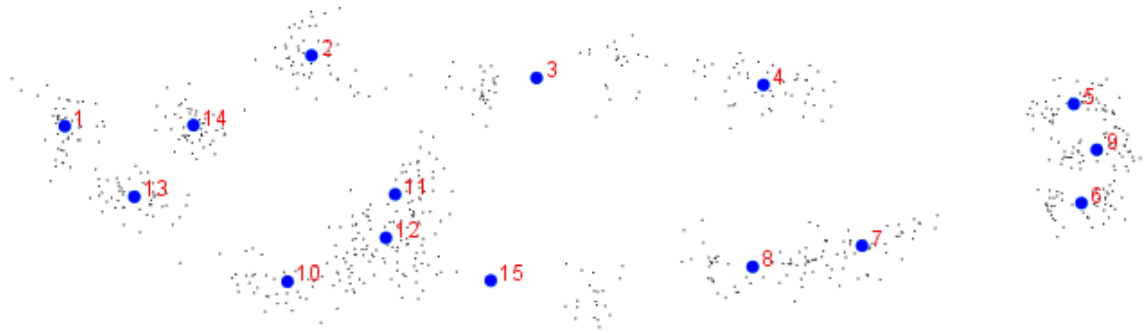


**Fig. 3 Overall consensus of all the landmark configurations** of the fish assemblage after procrustes superimposition in MorphoJ.

The raw landmark coordinates were superimposed by a General Procrustes Analysis (GPA, see overall consensus in Fig. 3). In this process, the landmark configurations minimize their variation in size, position and orientation. This method consists of three steps: translating all landmark configurations to the same centroid, scaling all configurations to unit centroid size, and rotating all configurations until the summed squared distances between the landmarks is minimum (Mitteröcker et al. 2013). The GPA was performed using the software MorphoJ v. 1.06d. After this process, the obtained procrustes landmark coordinates represent shape-only variables.

A Principal Component Analysis (PCA) was conducted on the procrustes landmark configurations in the program Past v. 3.14 to obtain principal components (PC). The PCs are vectors describing differences (variation) of specimen shape compared to the mean shape (consensus configuration) (Marramà et al. 2016b). A morphospace was built from PC1 and PC2 in Past v. 3.14.

Differences in shape along the axes of the morphospace (PCs) were visualized through thin-plate spline deformation grids (Mitteröcker et al. 2013) performed in the program tpsRelw v.1.56.

Centroid size, the square root of the summed squared distances of the landmarks (Mitteröcker et al. 2013), and indicator of overall size, was computed in tpsRelw v.1.56.

For a description of the tps series of software see Rohlf (2015).

The body length of all fishes was measured on photos from landmark 1 (Anterior tip of the mouth) to landmark 9 (Posterior margin of the caudal peduncle) using Adobe Photoshop CC 2014. Differences in the mean lengths between the two clusters were investigated with a two-sample t-test in PAST 3.14. Histogram and box-whisker plot for body lengths and centroid sizes were created also in PAST 3.14.

The area of the convex hull is defined as the amount of space occupied in the morphospace, representing the amount of shape variation of the fishes (Marramà et al. 2016b). The convex hull offers inside into the peripheral variability (what cluster gives more diversity to the assemblage; Farré et al. 2016) and is the smallest convex set with the most amount of reduction of empty space compared to cubes or spheres.

Kernel-density plots were created in PAST 3.14 using a Gaussian function to visualize areas of high (in red regions) or low (blue regions) density in the morphospace corresponding to spaces where taxa are clustered or dispersed (Farré et al. 2016; Marramà et al. 2016b).

Ripley's functions were created in PAST 2.12. It's another method to describe the spatial distribution pattern (random, uniform, or clustered) at both small and large distances (a point pattern may be random distributed at low distance and aggregated at large distance) (Werdelin & Lewis 2013; Marramà et al. 2016b).

Nearest neighbour analyses were performed in PAST 3.14 to estimate a convex hull area numerically and to interpret density and distribution behaviour of the inside Variability (e.g. clustered, even dispersed or random) inside the convex hull (Farré et al. 2016; Marramà et al. 2016b). An R value of $< 1$ indicates clustering between points, an $R \sim 1$ indicates randomization of points and an $R > 1$ indicates even dispersion (repulsion) of points. In nearest neighbour analysis, there is only one scale (Werdelin & Lewis 2013).

All these methods are based on the morphospace of the first two principal components.

# Results

The principal component analysis is summarised by 30 PC axes. The first three PCs together accounted for 82.53% of the total shape variation. The morphospace built on the first two PCs (see Fig. 4), revealed a differentiation into two clusters of fishes in the fish assemblage, which are called and marked as “red” and “blue” here. It should also be noted, that all specimens of the blue group have one dorsal fin, while all specimens of red group have two dorsal fins.

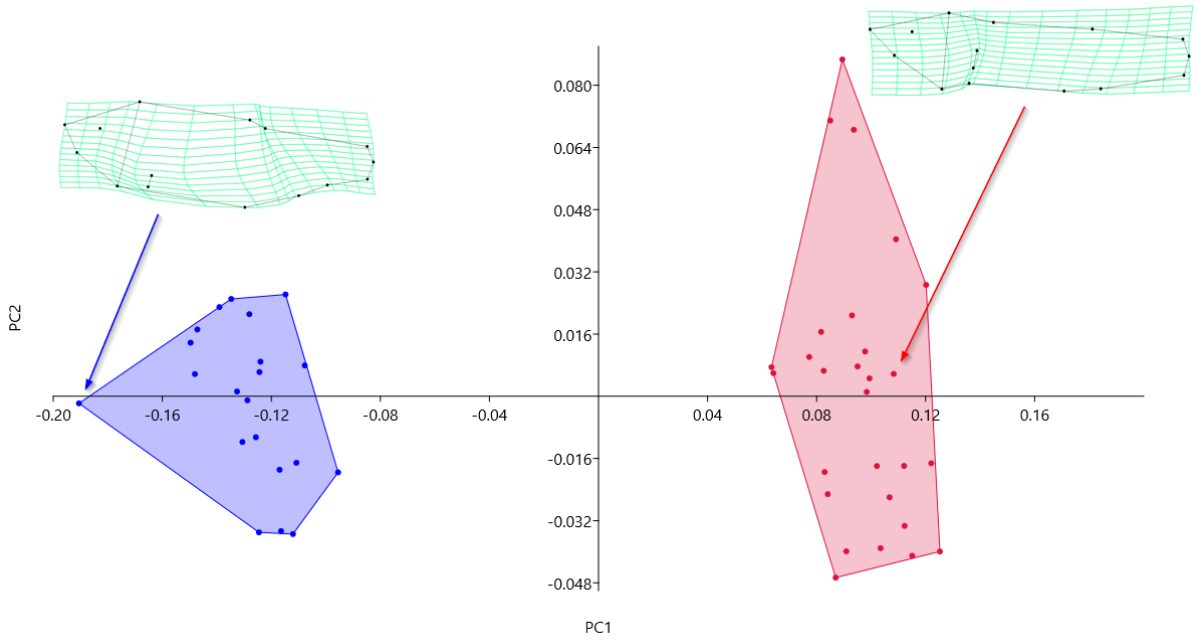


**Fig. 4 Morphospace built on principal component 1 and principal component 2** (n=49) with convex hulls (blue cluster represents specimens with one dorsal fin (n=21), red cluster represents specimens with two dorsal fins (n=28))

PC1 (73.63% % of total variance) describes mostly the variation in length and relative position of the dorsal fin (LM 3-4), the ventral-dorsal displacement of the pectoral fin (LM 11-12), the anterior-posterior displacement of the anal fin (LM 7-8), the shorting/lengthening of the caudal peduncle (LM 5-9-6) and the relative position of the pelvic fin (LM15) (see Fig. 5 and Fig. 6).

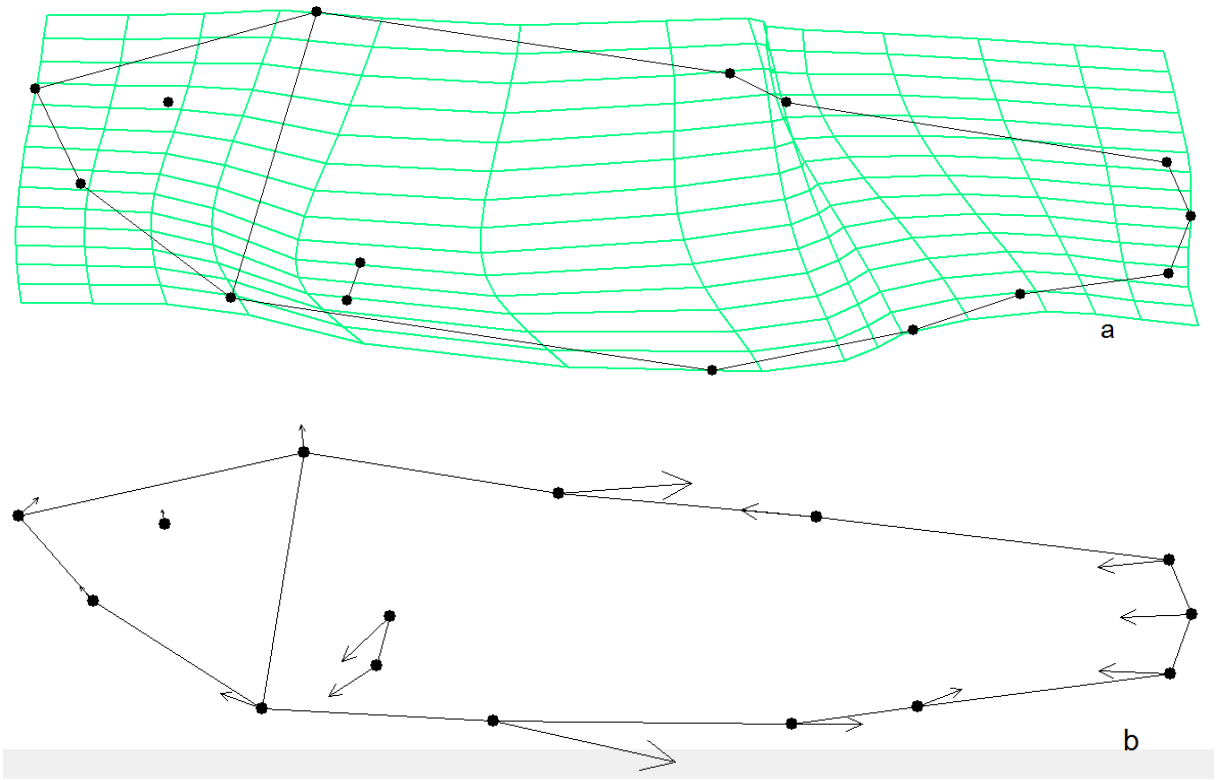


**Fig. 5 Shape changes along the negative scores of PC1.** a. Expressed as deformation grids; b. Expressed as vectors

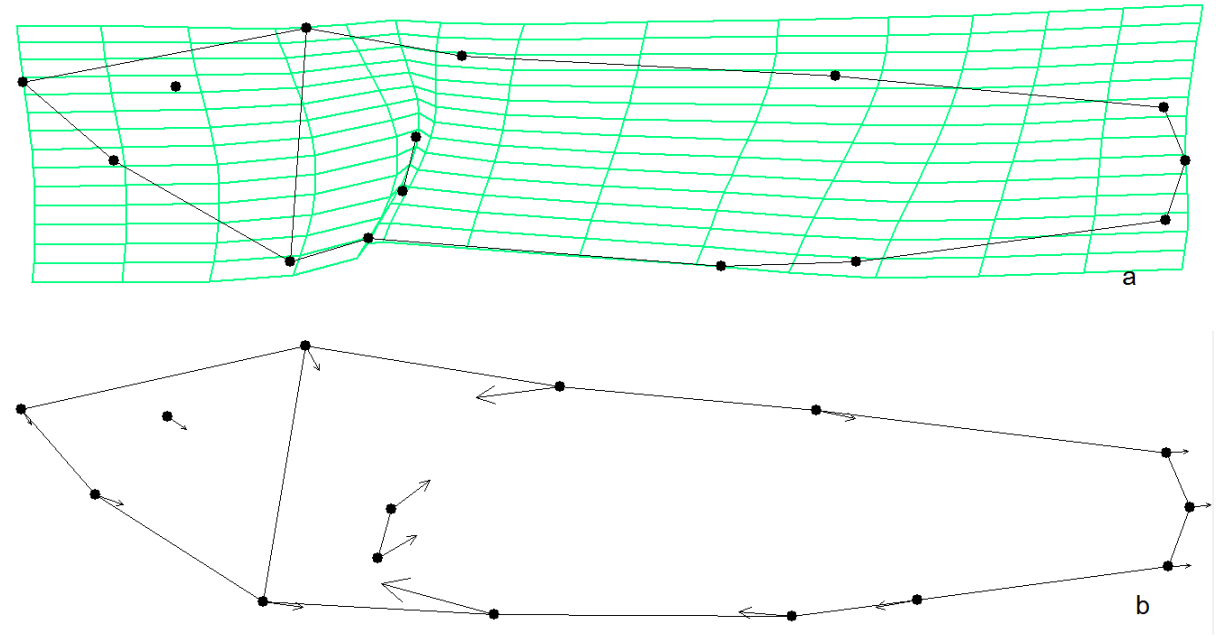


**Fig. 6 Shape changes along the negative scores of PC1.** a. Expressed as deformation grids; b. Expressed as vectors

The second PC (4.85% of total variance) does not actually show any variation related to shape but more or less an up- and downward arching of the body (see Fig. 7 and Fig. 8). Other PCs have no substantial impact, nor is it clear what they describe.

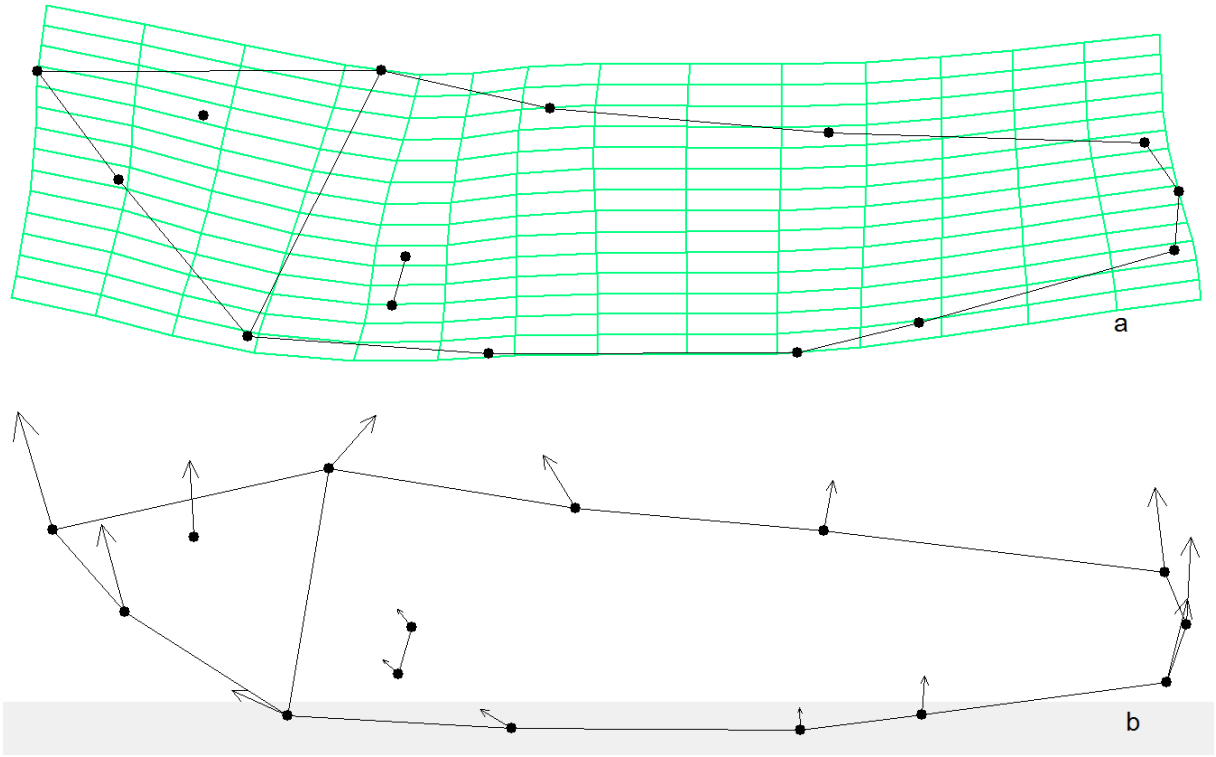


**Fig. 7 Shape changes along the positive scores of PC2.** a. Expressed as deformation grids; b. Expressed as vectors

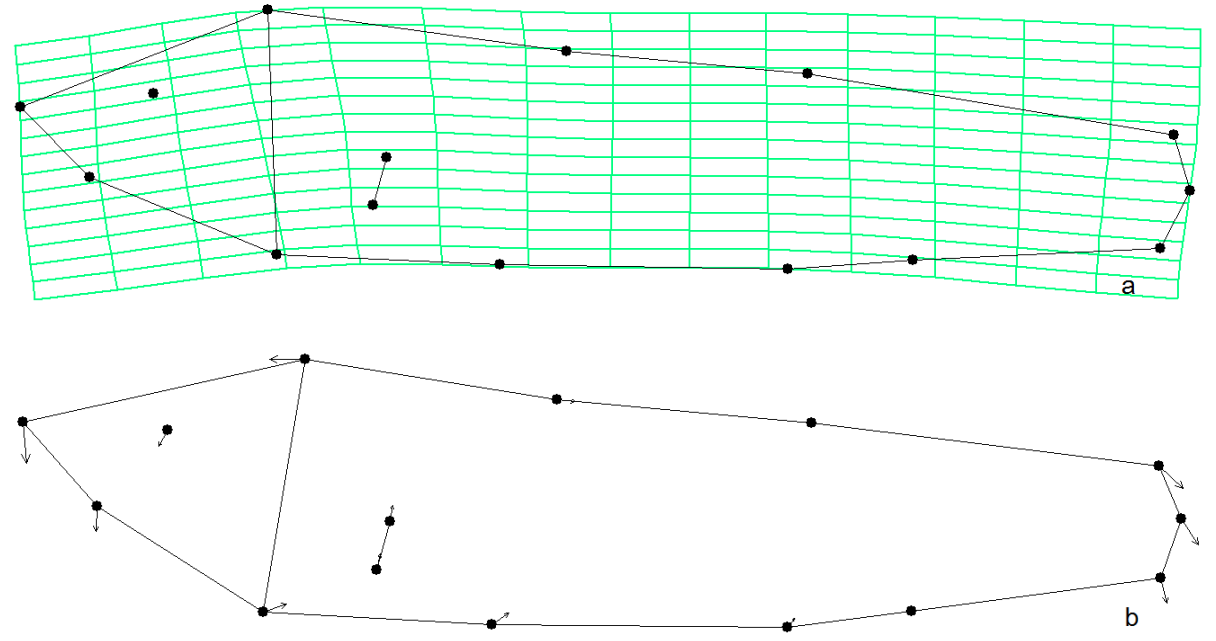


**Fig. 8 Shape changes along the negative scores of PC2.** a. Expressed as deformation grids; b. Expressed as vectors

As shown by the overall consensus shape for each cluster (computed separately; see Fig. 9 and 10), the fishes of the red cluster have their dorsal fin landmarks placed further apart. The pectoral fin is more in the center of the body, the anal fin located more anteriorly and the pelvic fin located near the head. Therefore, the specimens of the red cluster appear with a slender and elongated body-shape

and pointed head, whereas the fishes of the blue cluster have narrow placed dorsal fin landmarks, a more ventrally located pectoral fin, the anal fin placed more posteriorly, also the pelvic fin. Therefore, they appear more deep-bodied and shorter, while the head is more roundish.

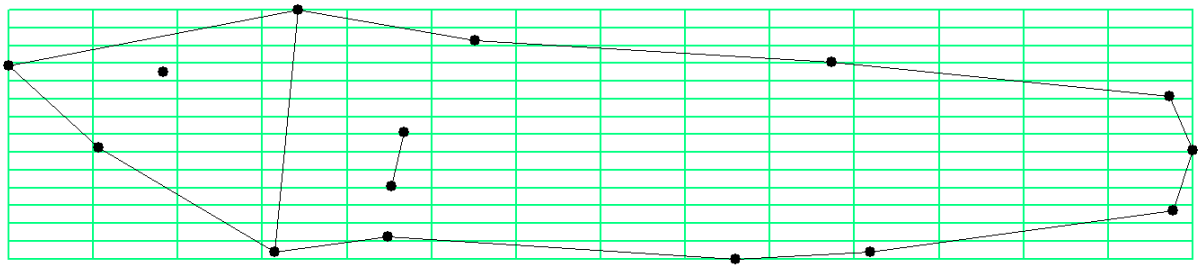

**Fig. 9 Overall consensus shape for the red cluster**, computed separated from the rest of the fish assemblage (n=28).

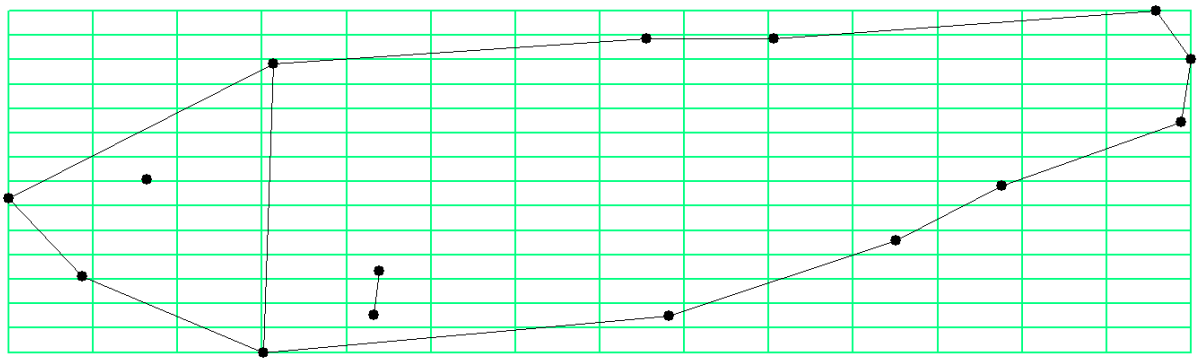

**Fig. 10 Overall consensus shape for the blue cluster**, computed separated from the rest of the fish assemblage (n=21).

As shown by the histogram in Fig. 11, the body length of the fishes range from 1.56 cm up to 13.8 cm and are 6.27 cm in the mean. Most of the fishes possess lengths of around 3 to 4.5 cm, while the fewest are around 7 to 8.5 cm. The histogram of the centroid size in Fig. 12 shows a similar distribution.

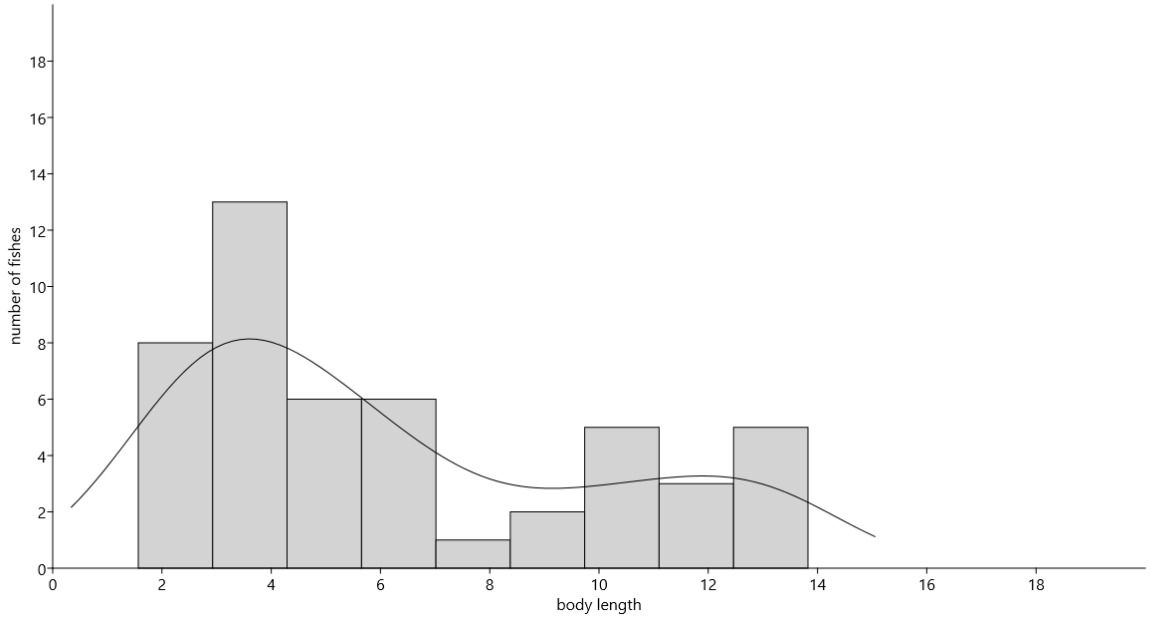


**Fig. 11 Histogram of the overall body length distribution of the fishes.** The line corresponds to the kernel density.

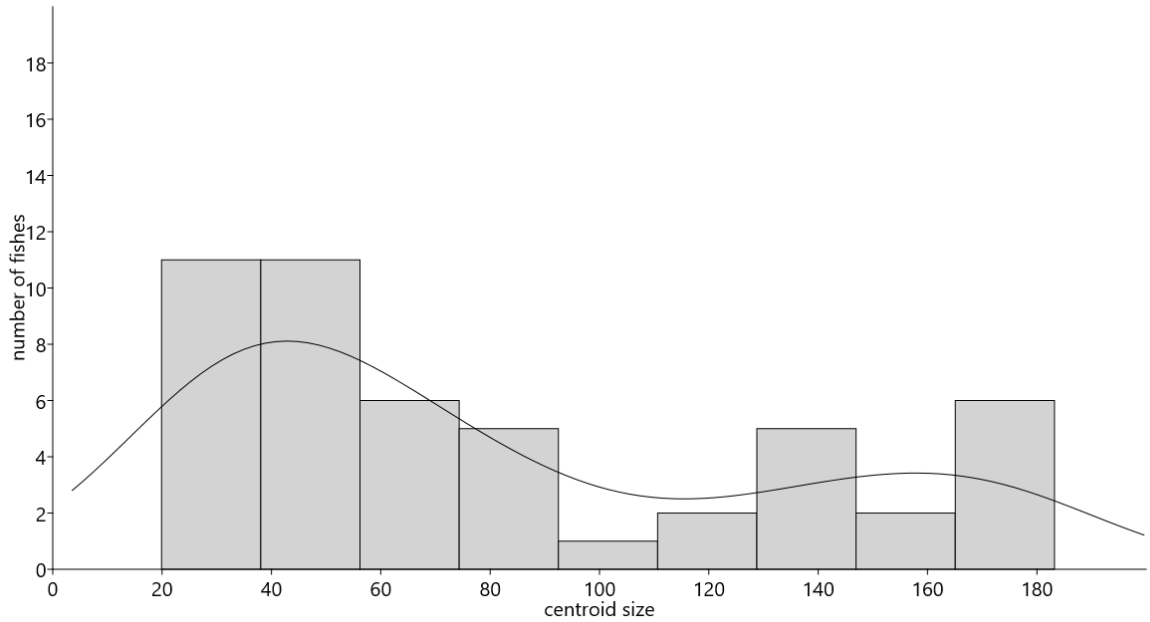


**Fig. 12 Histogram of the overall centroid size distribution of the fishes.** The line corresponds to the kernel density.

The fish clusters overlap in the box-plot of the body length (see Fig. 13) at around 5 to 6 cm, however, the mean body lengths between the red (n = 28; mean = 4.08 cm) and blue (n = 21; mean = 9.18 cm) fish cluster are significantly different (5.09 cm; $p<0.001$). Again, the box-plot of centroid size in Fig. 14

shows similar results. The centroid size significantly differs between means of the two clusters (75.041; $p<0.0001$).

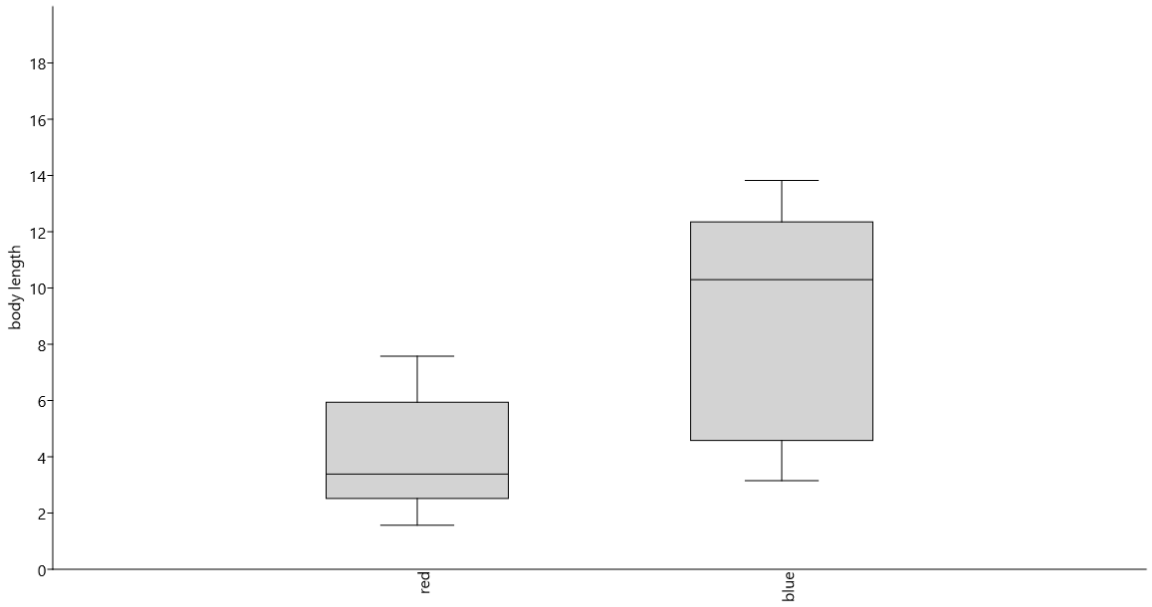


**Fig. 13 Box-whisker-plot of fish body lengths.** The horizontal line inside each box shows the median, while the minimum and maximum are shown as short horizontal lines ("whiskers").

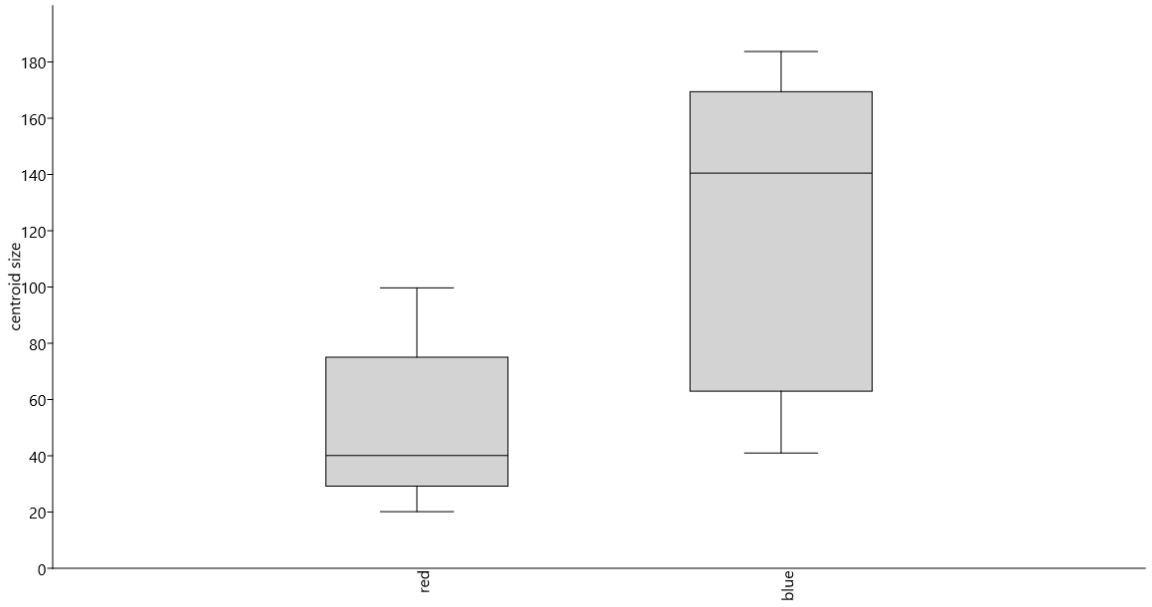


**Fig. 14 Box-whisker-plot of fish centroid size.** The horizontal line inside each box shows the median, while the minimum and maximum are shown as short horizontal lines ("whiskers").

The Kernel density plot that was built on the first two PCs (see Fig. 15A) shows two separated areas of high density (red-orange). The Ripley's function (Fig. 15B) values were higher than those corresponding to spatial randomness at all distances, thus confirming the presence of clusters in the morphospace of PC1 and PC2.

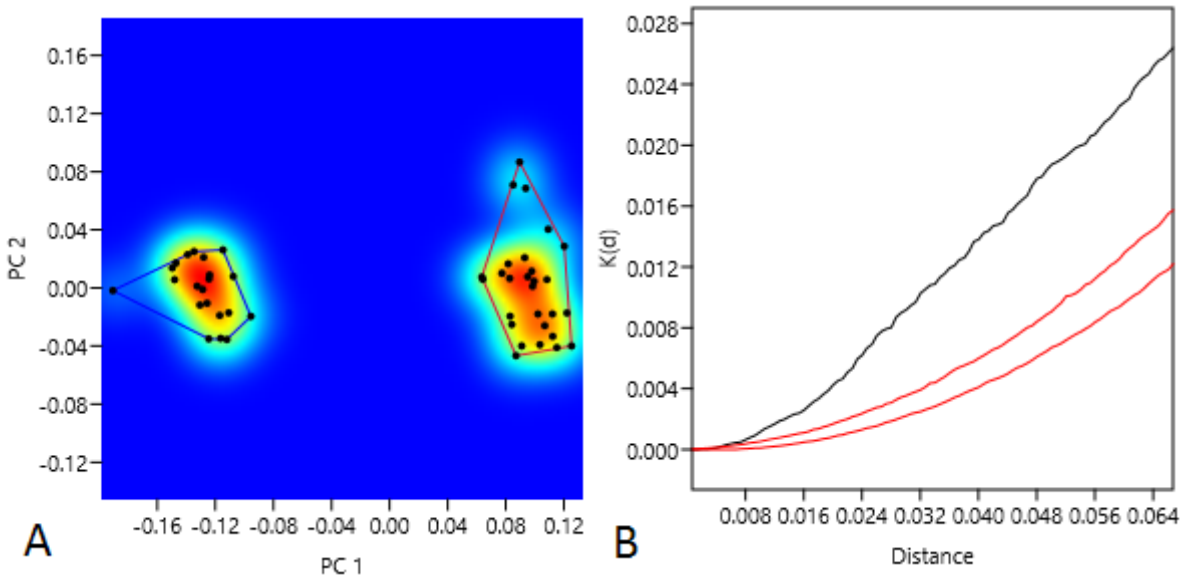


**Fig. 15 Point pattern analysis of the morphospace occupation of PC1 and PC2.** A. Kernel density plot. Two hotspots representing fishes from the blue (left) and red cluster (right). B. Ripley's K(d) analysis. The two red curves represent 95% confidence envelopes of the function; and the obtained curve is in black.

Looking closer into the inner point pattern of each cluster, the kernel density plot of the blue cluster in the fish assemblage (Fig. 16A) indicates several small hot spots with one specimen relatively separated from the rest of the group, along PC1. This is also confirmed by the Ripley's function (Fig. 16B), where specimens seem to be random distributed at lower distances, while aggregated at larger distances.

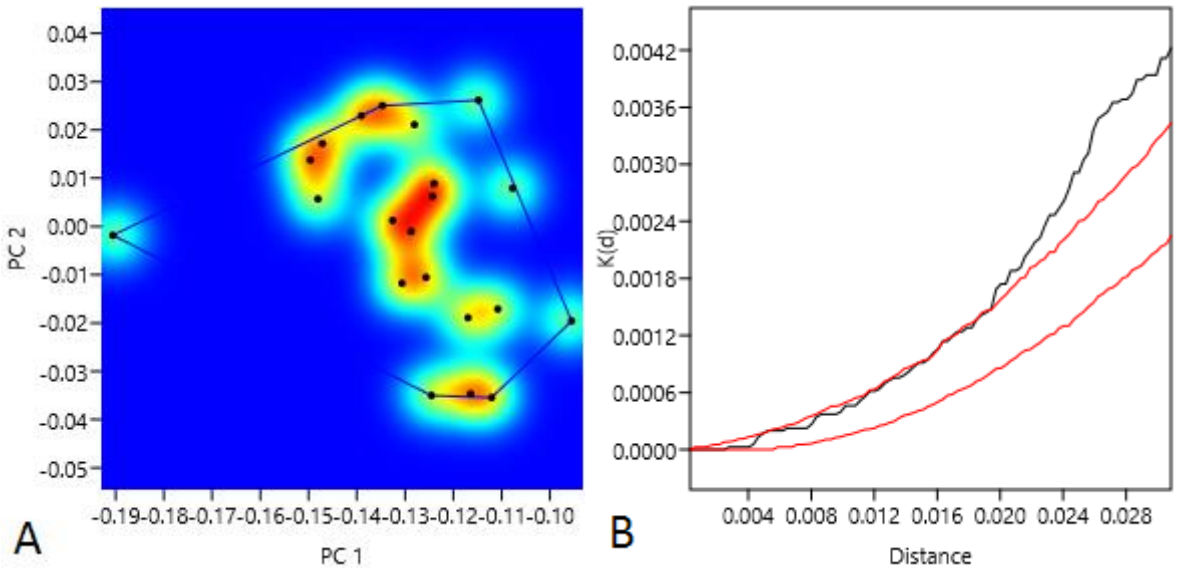


**Fig. 16 Point pattern analysis of the morphospace occupation of PC1 and PC2 of the blue cluster.** A. Kernel density plot with several minor hot spots. B. Ripley's K(d) analysis. The two red curves represent 95% confidence envelopes of the function; and the obtained curve is in black.

In the red cluster, the kernel density plot (Fig. 17A) shows several minor hot spots with three specimens separated along PC2. Ripley's function of the red cluster (Fig. 17B) indicates a random distribution at low distances and critical bordering and switching from random to aggregated at larger distances.

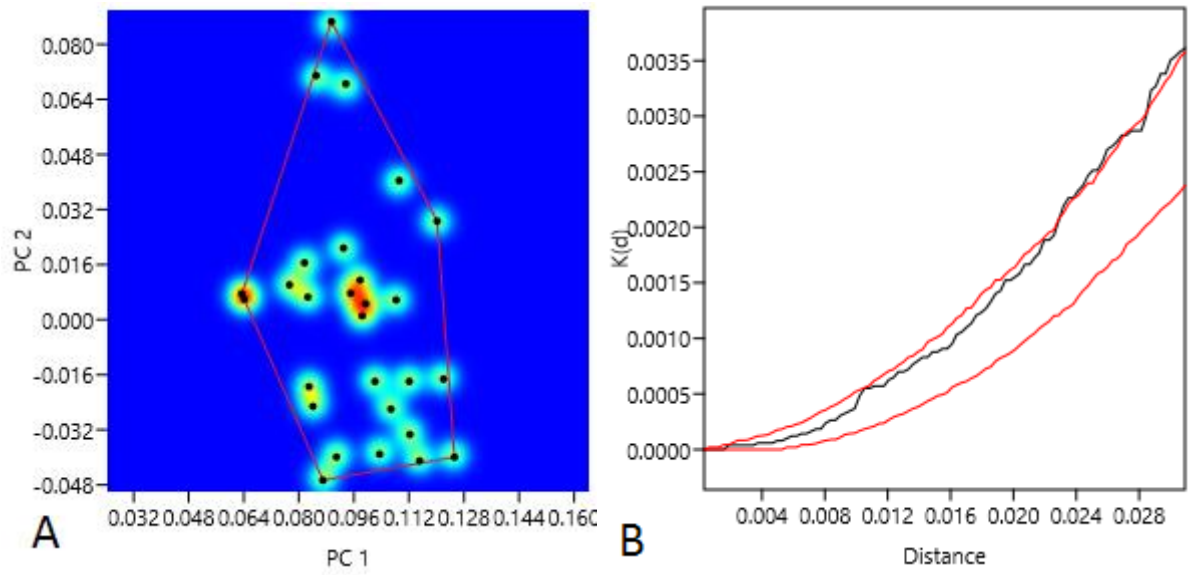


**Fig. 17 Point pattern analysis of the morphospace occupation of PC1 and PC2 of the red cluster.** A. Kernel density plot with several minor hot spots. B. Ripley's K(d) analysis. The two red curves represent 95% confidence envelopes of the function; and the obtained curve is in black.

The nearest neighbour analysis of PC1 and PC2 (Table 1) also shows that the fish assemblage appears significantly clustered (all: p(random)=0.00047), rejecting the null hypothesis of random distribution

in the morphospace. However, specimens within the clusters are suggested to be randomly distributed by nearest neighbour analysis (blue cluster: p(random)=0.86591; red cluster: p(random)=0.27718). The red cluster appears to a wider convex hull area, while the blue cluster is denser in distribution.

**Table 1 Basic statistics and results of the nearest neighbour analysis built on the first two PCs.** An R-value below 1 indicates significant attraction between points; an R-value above 1 indicated significant repulsion between points.

| | **all** | **blue cluster** | **red cluster** |
|---|---|---|---|
| N | 49 | 21 | 28 |
| Area | 0.02642 | 0.0033335 | 0.0050839 |
| Mean density | 1854.1 | 6299.6 | 5507.6 |
| Mean distance | 0.0073248 | 0.0061783 | 0.0074606 |
| Expected distance | 0.01161 | 0.0062996 | 0.0067373 |
| Z | -4.9428 | -0.16886 | 1.0867 |
| p(random) | 0.00047561 | 0.86591 | 0.27718 |
| R | 0.6309 | 0.98074 | 1.1073 |

# Discussion

Several problems occurred while attempting to assess the fossil material with geometric morphometrics. When setting landmarks, specimens were often incomplete, lacking the head, the caudal region or even both and only the middle part was preserved (see Fig. 18 for an example). Even when a specimen was missing only one landmark point, like the tip of the snout or a part of the dorsal fin, it had to be excluded from the analysis.

**Fig. 18 Specimen lacking parts of the head region**, therefore missing 3 landmarks.

As long as this bad preservation is no species related phenomenon, there should be no bias from excluding these specimens from the dataset.

There are a couple of methods to deal with missing landmarks. However, most of them base and rely on bilateral symmetry (i.e. reflected relabeling; Gunz et al. 2009), and requires virtual reconstruction of the damaged or distorted fossils. If landmarks are missing on both sides, positions are estimated by minimizing the thin-plate spline bending energy (e.g. Gunz et al. 2009; Adams & Otárello-Castillo 2013).

There is, for instance, a missing landmark function in the program tpsDig2. However, using this technique for further analysis like PCA will aggregate specimens with the same missing landmarks together, while also separating them from other specimens that should be actually near them (see Fig. 19). Therefore, it does not indicate any variation in actual shape.

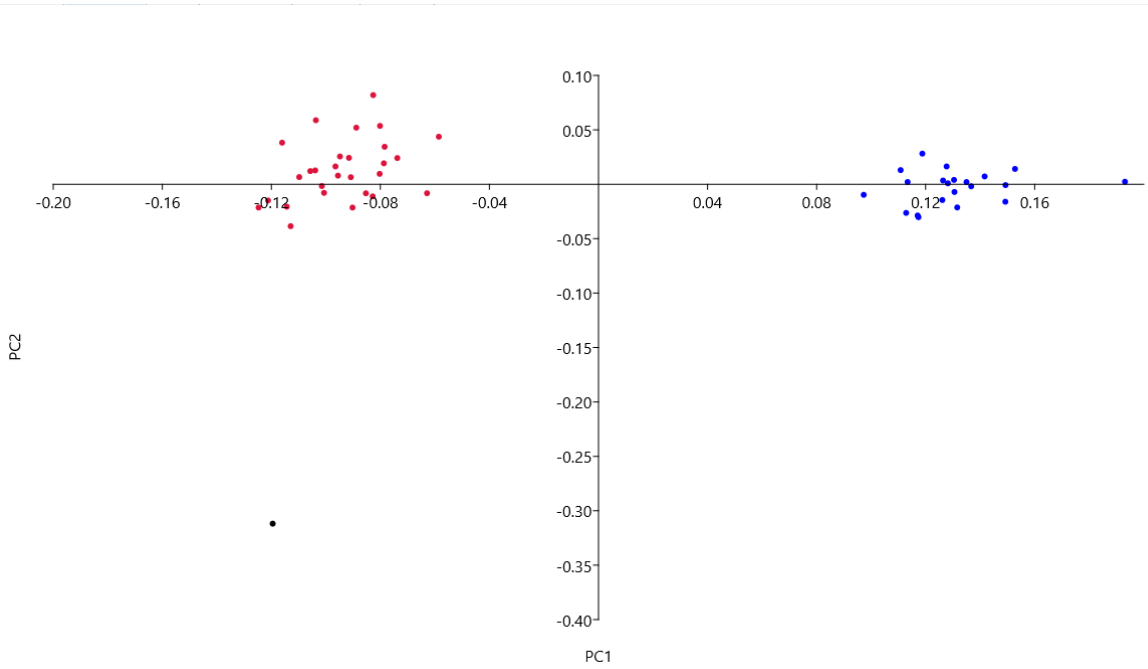


**Fig. 19 Morphospace built on PC1 and PC2 with the specimen of Fig. 18** (n=50). The black spot that is separated from the two clusters represents the specimen with three missing Landmarks.

Creating thin-plate splines using this method also leads to distortion of the deformation-grid frame (see Fig. 20). Other programs are most likely required to create usable results.

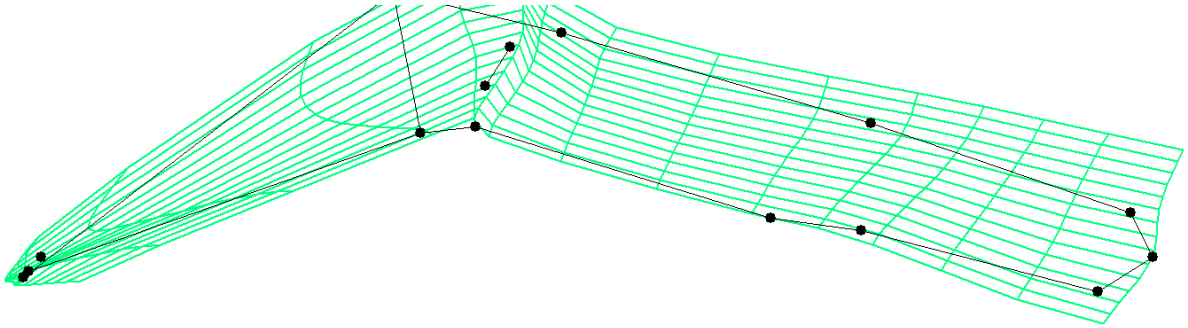

**Fig. 20 Distorted thin-plate spline deformation grid in tpsRelw** of the specimen with missing landmarks on the head using missing landmark function in tpsDig2. (The graphic is cut-off at the upper part due to a displaying error in the program tpsRelw)

A lot of specimens had to be excluded from the analysis leading to a reduction in the total number of analysed fossils from over 200 to 49. A balance between the number of landmarks, enough to capture sufficient information of the body shape and the number of excluded specimens, resulting from an inaccessibility of landmarks to maximise sample size, had to be found.

Furthermore, some specimens that were extremely bended, twisted or deformed due to taphonomic processes had to be excluded from the analysis in order not to mislead the statistics into wrong

conclusions. Sometimes the textures of the fossils were also extremely blurred or covered important parts on the photos, which were therefore hard to recognize and made landmark setting difficult.

Another problem was that the fishes possessed either one or two dorsal fins. Defining the number and positions of homologous landmarks between organisms is difficult using landmark-based analyses, since different criteria can influence results (Farré et al. 2016). Furthermore, the position and number of body fins is a critical taxonomical criterion (Nelson 2006). In this case it is not clear whether the single dorsal fin of species A is a homologous structure to the first, second or both dorsal fins of species B. Some studies solved this problem by putting the first landmark on the anterior position of the first dorsal fin and a second landmark on the posterior position of the second dorsal fin (e.g. Farré et al., 2016), which was also done in this study. Others put two landmarks on the anterior and posterior position of the first dorsal fin and two landmarks in the same way on the second dorsal fin and probably marking those landmarks missing if only one dorsal fin existed (see Farré et al. 2016). This was not tested because of the above mentioned problem of erroneous results from the use of the missing landmark function in tpsDig2. Another method is to place a semi-landmark between the first and second landmark on the dorsal fin to mark if a second dorsal fin is present or absent (see Farré et al. 2016; Lombarte et al. 2016), which should not make a difference in the computing of the PCA but surely is helpful when looking at the shape.

The first PC was helpful to separate the fish assemblage into two clusters and described by far the most variation to all the other axes (73.63%). The second PC with the second most variance (4.86%) was related to an up- and downward arching of the body which Carpenter (1996) called an “arching effect” of fish bodies and he suggested that this might be a measurement artefact, resulting from problems in the preservation of the specimens or instead may have a functional explanation. Valentin et al. (2008) suggested that this is due to slight posture differences between fishes during landmark capture. However, since the fossils presented here are rigid structures and incapable of flexing, it is expected that this arching is to be a post mortem effect, captured during fossilisation.

The other axes can more or less be ignored since their impact is only marginal. It should also be noted that the only resulting PC axis that is likely to actually represent a biological phenomenon is PC1 because all subsequent axes are constrained by being orthogonal to the first axis (Cooke & Terhune 2015). Therefore, shape variation is explained by the length and position of the dorsal fin, the relative position of the pectoral, anal and pelvic fin plus the length of the caudal peduncle region.

In the overall consensus for each cluster (see Fig. 9 and 10), one can see that fishes of the red cluster possess bodies of a slender, elongated shape with pointed heads while fishes of the blue cluster are more deep-bodied with rounder heads. Some of the shape differences between the two clusters analysed here could be given a functional interpretation. In freshwater communities, piscivorous

species tend to be more elongated than deeper-bodied benthic foragers (Cavalcanti et al. 1999). The relationship between morphology and ecology in fishes have long been known, so that it might be possible to predict ecological patterns from patterns in the morphospace (Cavalcanti et al. 1999), because environments constrain both morphology and ecology (Recasens et al. 2006). However, a space describing shape variation does not always describe a difference in functionality, since different geometries can be functionally equivalent (Marramà et al 2016a). Furthermore, landmarks describing the total body shape do not only capture meaningful aspects of biomechanics but shape may also be the result of phylogeny, allometry or other factors (Cooke & Terhune 2015). Therefore, it would be necessary to capture only functional aspects of shape, not whole body shape aspects to interpret real functionality.

In this context, the convex hulls here should not be interpreted as a measure for functional diversity, but as the amount of shape variation occupied by each cluster in the morphospace.

Centroid size as well as body length was used to compare the size of the two clusters. Although centroid size seems to be the favourite measurement for overall body size, the results suggested that centroid size and body length were highly similar. However, centroid size is a dimensionless quantity, making it hard for the visual interpretation. Therefore, body length is in this case the preferable measurement for size since adding a dimension component makes it more intuitive. Plus, body length may also be tied more directly to size and be functionally relevant (Cooke & Terhune 2015).

The Kernel density plot presented a direct visual image of the density distribution behaviour of the fish assemblage in the morphospace of PC1 and PC2. The fishes were aggregated into two clusters of high density. When looking deeper into the inside distribution behaviour of each cluster, the distribution seems to be random however. In the blue cluster there is one specimen separated from the rest of the group, along PC1, that could actually represent a highly variable specimen or another species. Fishes in the red cluster have three specimen separated from the rest of the group, but along PC2 and is therefore probably just a strongly arching effect.

The Ripley's function provided another visual presentation of the distribution behaviour of the fish assemblage in the morphospace of PC1 and PC2. It confirmed the results of the kernel density that the fish assemblage is aggregated in two clusters and that specimens within both clusters are randomly distributed. However, at large distances, specimens seem to be almost in an aggregated state within both clusters.

The nearest neighbour analysis provided numerical data of convex hull area, density and also a statistical presentation of distribution behaviour, which is clustered on large scale (the fish assemblage) and random on low scale (within clusters), thus confirming the results of the other analyses.

When the study started, it was expected to see a diversification into all the inherent taxa of the fish assemblage in the morphospace or at least into the three suggested taxa of *Gobius*, *Leuciscus* and *Morone*. The shape analysis, however, separated the fish assemblage in only two clusters. The shape variation within both clusters is randomly distributed, suggesting that specimens could be from the same taxon, a family of closely related taxa or may just share a similar body shape. Whether the first, second or third is the case is not possible to say just from the morphometrics.

After identifying some of the specimens based on morphological key traits, it became obvious, that the fishes belong to *Gobius*, *Leuciscus* and also other taxa. The blue cluster contains specimens of *Leuciscus*, based on the fact that all the specimens in this cluster possess one dorsal fin. The red cluster contains specimens of *Gobius*, based on the fact that all the specimens in this cluster possess two dorsal fins. *Morone* may be in the assemblage, but not all the specimens of the assemblage were identified and it is possible that *Morone* is not so abundant in Schaßbach, since the brackish influence is low.

One specimen was identified in the fish assemblage that seems to be a predator type, based on its teeth. However, it does neither belong to *Morone,* nor to *Gobius*, because it only has one dorsal fin. It does also not belong to *Leuciscus*, but it has a similar shape and was therefore grouped to the blue cluster in the morphospace. This indicates that the geometric morphometric analysis that is based on body shape was unable to fully separate all the taxa in the assemblage. A similarity in body shape does not necessarily indicate a common phylogeny. It can mean, however, that these specimens are adapted to the same environmental constraints. This is interesting, because geometric morphometrics is often used as a tool for taxon classification and can be, in this case, questioned. Especially when used on assemblages of unknown taxa.

# References


Adams, D. C., & Otárello-Castillo, E. (2013). geomorph: an r package for the collection and analysis of geometric morphometric shape data. *Methods in Ecology and Evolution*, *4*(4), 393–399.

Beck-Managetta, P. (1952). Zur Geologie und Paläontologie des Tertiärs des unteren Lavanttales. *Jahrbuch Der Geologischen Bundesanstalt Wien*, *95*, 1–102.

Carpenter, K. E. (1996). Morphometric Pattern and Feeding mode in Emperor Fishes (Lethrinidae, Perciformes). *Advances in Morphometrics*, *284*, 479–487.

Cavalcanti, M., Monteiro, R. L., & Lopes, P. R. D. (1999). Landmark-based Morphometric Analysis in Selected Species of Serranid Fishes ( Perciformes : Teleostei ) Landmark-based Morphometric Analysis in Selected Species of. *Zoological Studies*, *38*(3), 287–294.

Clabaut, C., Bunje, P. M., Salzburger, W., & Meyer, A. (2007). Geometric morphometric analyses provide evidence for the adaptive character of the Tanganyikan cichlid fish radiations. *Evolution*, *61*(3), 560–578.

Cooke, S. B., & Terhune, C. E. (2015). Form , Function , and Geometric Morphometrics. *The Anatomical Record*, *298*(1), 5–28. http://doi.org/10.1002/ar.23065

Farré, M., Tuset, V. M., Maynou, F., & Lombarte, A. (2016). Selection of landmarks and semilandmarks in fishes for geometric morphometric analyses in ecological studies : a comparative from analytical methods. *Scientia Marina*, *80*(2), 1–12. http://doi.org/10.3989/scimar.04280.15A

Geologische Bundesanstalt Wien. (2014a). Exkursionspunkt 4 : Schönweg. *Berichte Der Geologischen Bundesanstalt*, *105*, 39–40.

Geologische Bundesanstalt Wien. (2014b). Exkursionspunkt 5 : Oberaigen. *Berichte Der Geologischen Bundesanstalt*, *105*, 41–42.

Gunz, P., Mitteroecker, P., Neubauer, S., Weber, G. W., & Bookstein, F. L. (2009). Principles for the Virtual Reconstruction of Hominin Crania. *Journal of Human Evolution*, *57*(1), 48–62.

Harzhauser, M., Mandic, O., Neubauer, T. A., Georgopoulou, E., Hassler, A., & Harzhauser, M. (2015). Disjunct distribution of the Miocene limpet-like freshwater gastropod genus Delminiella. *Journal of Molluscian Studies*, 1–8. http://doi.org/10.1093/mollus/eyv040

Klingenberg, C. P., Barluenga, M., & Meyer, A. (2003). Body shape variation in cichlid fishes of the Amphilophus citrinellus species complex. *Biological Journal of the Linnean Society*, *80*(3), 397–408.

Lombarte, A., Gordoa, A., Whitfield, A. K., James, N. C., & Tuset, V. M. (2016). Ecomorphological analysis as a complementary tool to detect changes in fish communities following major perturbations in two South African estuarine systems. *Environmental Biology of Fishes*, *94*(4), 601–614. http://doi.org/10.1007/s10641-011-9966-0

Marramà, G., Garbelli, C., & Carnevale, G. (2016a). A clade-level morphospace for the Eocene fishes of Bolca : Patterns and relationships with modern tropical shallow marine assemblages. *Bollettino Della Società Paleontologica Italiana*, *55*(2), 139–156. http://doi.org/10.4435/BSPI.2016.13

Marramà, G., Garbelli, C., & Carnevale, G. (2016b). A morphospace for the Eocene fish assemblage of Bolca , Italy : A window into the diversification and ecological rise to dominance of modern tropical marine fishes. *Bollettino Della Societa Paleontologica Italiana*, *55*(1), 11–21. http://doi.org/10.4435/BSPI.2016.02

Meller, B., Zetter, R., Hassler, A., Bouchal, J. M., Hofmann, C.-C., & Grímson, F. (2015). Middle Miocene macrofloral elements from the Lavanttal Basin, Austria, Part I. Ginkgo adiantoides (Unger) Heer. *Austrian Journal of Earth Sciences*, *108*(2), 185–198. http://doi.org/10.17738/ajes.2015.0020

Mitteröcker, P., Gunz, P., Windhager, S., & Schaefer, K. (2013). A brief review of shape , form , and allometry in geometric morphometrics , with applications to human facial morphology. *Hystrix, the Italian Journal of Mammalogy*, *24*(1), 59–66. http://doi.org/10.4404/hystrix-24.1-6369

Nelson, J. S. (2006). *Fishes of the World* (Vol. Fourth Edi). John Wiley & Sons, New Jersey.

Nolf, D., & Brzobohatý, R. (2009). Lower Badenian fish otoliths of the Styrian and Lavanttal basins, with a revision of Weinfurter's type material. *Annalen Des Naturhistorischen Museums in Wien*, *111 A*(1), 323–356.

Recasens, L., Lombarte, A., & Sánchez, P. (2006). Teleostean fish assemblages in an artificial reef and a natural rocky area in Catalonia (Northwestern Mediterranean): An ecomorphological approach. *Bulletin of Marine Science*, *78*(1), 71–82.

Reischenbacher, D., Refelj, H., Sachsenhofer, R. F., Jelen, B., Ćorić, S., Gross, M., & Reichenbacher, B. (2007). Early Badenian paleoenvironment in the Lavanttal Basin (Mühdorf Formation; Austria): Evidence from geochemistry and paleontology. *Austrian Journal of Earth Sciences*, *100*, 202–229.

Reischenbacher, D., & Sachsenhofer, R. F. (2013). Basin formation during the post-collisional evolution of the Eastern Alps: the example of the Lavanttal Basin. *International Journal of Earth*

*Sciences*, *102*(2), 517–543. http://doi.org/10.1007/s00531-012-0807-y

Rohlf, J. (2015). The tps series of software. *Hystrix*, *26*(1), 1–4.

Valentin, A., Penin, X., Chanut, J.-P., Sévigny, J. -M., & Rohl, F. J. (2008). Arching effect on fish body shape in geometric morphometric studies. *Journal of Fish Biology*, *73*(3), 623–638. http://doi.org/10.1111/j.1095-8649.2008.01961.x

Werdelin, L., & Lewis, M. (2013). Temporal Change in Functional Richness and Evenness in the Eastern African Plio-Pleistocene Carnivoran Guild. *PLoS ONE*, *8*(3), e57944. http://doi.org/10.1371/journal.pone.0057944

Zelditch, M. L., Swiderski, D. L., Sheets, H. D., & Fink, W. L. (2004). Geometric morphometrics for biologists: a primer. *Elsevier Academic Press*, 437.